J. Fluid Mech. (1988), *vol.* 192, *pp.* 17–31
Printed in Great Britain

Excitation of long internal waves by groups of short surface waves incident on a barrier

By YEHUDA AGNON
Department of Mathematics, MIT, Cambridge, MA 02139, USA

AND CHIANG C. MEI
Department of Civil Engineering, MIT, Cambridge, MA 02139, USA

(Received 17 July 1987)

The effects of diffraction by a long barrier on second-order long waves forced by sinusoidally modulated short incident waves are examined for a two-layered model ocean. When the group velocity of the short waves lies between the phase velocities of the longest baroclinic and barotropic modes, long internal waves of the frequency equal to twice the modulational frequency of the short waves are found to radiate away from the edge ray which divides the geometrical shadow and the illuminated region. In particular the baroclinic wave can penetrate the shadow. This penetration occurs when the internal long wave is not resonated by short surface waves.

1. Introduction

It is well known that surface waves can interact nonlinearly to produce internal waves. Past research on this topic has been concentrated on the resonant interaction of two surface-wave components with an internal wave mode in an open sea without interruption by a scatterer. Typical of these studies are Ball (1964), Thorpe (1966), Lewis, Lake & Ko (1974), Joyce (1974), and Dysthe & Das (1981). In this paper we report an investigation of the added effect of a scatterer. The physical motivation is to see whether long waves caused by the interaction of short waves can penetrate zones which are sheltered from short waves. As an illustration we select a thin and straight barrier extending from $y = 0$ to ∞, attacked by slowly and sinusoidally modulated surface waves incident normally in the positive x-direction as sketched in figure 1. From geometrical optics for infinitesimal waves, we expect that the first quadrant in the horizontal (x, y)-plane is a shadow zone free of short waves, the second quadrant has incident and normally reflected waves of equal amplitudes, and the third and fourth quadrants have only the incident waves. Because of the slow modulation, second-order set-downs are forced. These are long waves with a frequency twice the modulational frequency of the short waves and propagate in the same direction as, and at the group velocity C_g of, the short wavetrains. Relative to the long wave scale, the short waves change suddenly across the x-axis, and so do these set-downs. Physical requirement for smoothness can be met only if additional free waves of the same long period are radiated from the x-axis on both sides of the breakwater. They consist of both surface (barotropic) and internal (baroclinic) modes each with its own phase velocity U_S and U_I respectively. If $U_I < C_g < U_S$, the free internal waves must propagate in directions different from those of all other waves and can enter the shadow behind the barrier.

In this paper we describe a quantitative theory for this second-order phenomenon

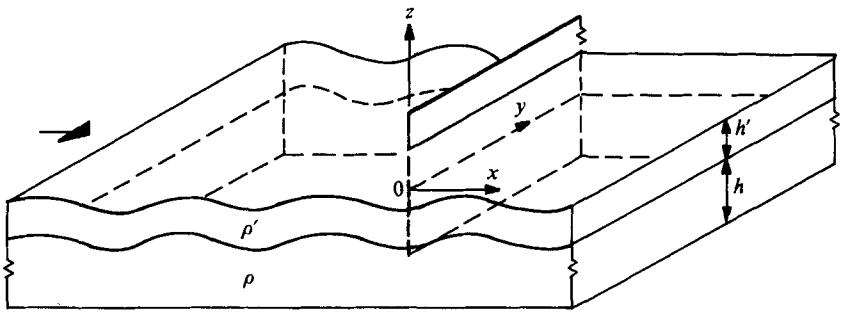

FIGURE 1. A barrier in a two-layered sea.

in a two-layered fluid. We first discuss the second-order set-downs locked to simple progressive waves, then the diffraction boundary layers around the edges (the x-axis) of the shadow and the reflection zones. In these boundary layers, correction to geometrical optics for diffraction of the short waves is made with the help of the parabolic approximation. However, it will be shown that these boundary layers are only of local importance for providing a smooth transition, and the second-order long waves on either side of the transition can be matched directly. In particular the amplitude of internal long waves propagating into the shadow of the barrier is determined.

2. The nonlinear governing equations

Consider a two-layer fluid with the lower layer of density ρ and static depth h, and the upper layer of density ρ' and static depth h'. The origin of the coordinate system is chosen at the static interface between the two layers with the z-axis pointing upwards. The full nonlinear equations for the velocity potential in the upper layer and the free surface displacement ζ' are

$$\Phi'_{xx}+\Phi'_{yy}+\Phi'_{zz}=0 \quad (\zeta<z<\zeta'+h'), \tag{2.1}$$

$$\zeta'_t+\Phi'_x\zeta'_x+\Phi'_y\zeta'_y=\Phi'_z \quad (z=\zeta'+h'), \tag{2.2}$$

$$\Phi'_t+g\zeta'+\tfrac{1}{2}(\Phi'^2_x+\Phi'^2_y+\Phi'^2_z)=0 \quad (z=\zeta'+h'). \tag{2.3}$$

In the lower layer the governing equations are

$$\Phi_{xx}+\Phi_{yy}+\Phi_{zz}=0 \quad (-h<z<\zeta), \tag{2.4}$$

$$\Phi_z=0 \quad (z=-h). \tag{2.5}$$

At the interface $z=\zeta$, the boundary conditions are

$$\zeta_t=\Phi_z-\Phi_x\zeta_x-\Phi_y\zeta_y=\Phi'_z-\Phi'_x\zeta_x-\Phi'_y\zeta_y, \tag{2.6}$$

$$\rho[\Phi_t+g\zeta+\tfrac{1}{2}(\Phi_x^2+\Phi_y^2+\Phi_z^2)]=\rho'[\Phi'_t+g\zeta+\tfrac{1}{2}(\Phi'^2_x+\Phi'^2_y+\Phi'^2_z)]. \tag{2.7}$$

On both sides of the barrier, the x-component of the velocity in both layers must vanish. Far away from the tip of the barrier, the radiation condition must be satisfied.

Let ω be the frequency of the short waves, ϵ be the measure of the small-wave slope

and Ω be the modulational frequency which is of the order $\epsilon\omega$. The solution can be sought in terms of multiple-scale expansions:

$$\Phi = \sum_{n=1}^{\infty} \epsilon^n \sum_{m=-n}^{n} \phi_{nm} \, \mathrm{e}^{-\mathrm{i}m\omega t}, \tag{2.8}$$

$$\zeta = \sum_{n=1}^{\infty} \epsilon^n \sum_{m=-n}^{n} \zeta_{nm} \, \mathrm{e}^{-\mathrm{i}m\omega t}, \tag{2.9}$$

where $$\phi_{nm}(x, y, z, x_1, y_1, t_1) = \phi^*_{n,-m}, \quad \zeta_{nm}(x, y, x_1, y_1, t_1) = \zeta^*_{n,-m}, \tag{2.10}$$

with $$x_1 = \epsilon x, \quad y_1 = \epsilon y, \quad t_1 = \epsilon t. \tag{2.11}$$

The superscript (*) denotes the complex conjugate. By Taylor expansion around the static free surface at $z = h'$ and also around the static interface at $z = 0$, and by using the assumed expansions, one gets a sequence of perturbation problems for each set of indices (n, m). We note that the potentials ϕ_{11}, ϕ'_{11} and the displacements ζ_{11}, ζ'_{11} correspond to the first-order short waves, while the potentials ϕ_{10}, ϕ'_{10} and displacements ζ_{20}, ζ'_{20} correspond to the second-order long waves.

For later use we first recall from standard literature (e.g. Lamb 1932, p. 372) some elementary results for simple progressive waves at the first order. The potentials in the two layers are

$$\phi_{11} = A_0 f(z) \, \mathrm{e}^{\mathrm{i}kx} \equiv A_0 \cosh k(z+h) \, \mathrm{e}^{\mathrm{i}kx} \quad (-h < z < 0), \tag{2.12}$$

$$\phi'_{11} = A_0 f'(z) \, \mathrm{e}^{\mathrm{i}kx} \equiv A_0 (C \cosh kz + B \sinh kz) \, \mathrm{e}^{\mathrm{i}kx} \quad (0 < z < h'), \tag{2.13}$$

where $$B = \sinh kh, \quad C = \left(\frac{\rho}{\rho'}\right) \cosh kh - \left(\frac{gk}{\omega^2}\right) \frac{\rho - \rho'}{\rho'} \sinh kh. \tag{2.14}$$

The free surface and the interface displacements are

$$\zeta'_{11} = \tfrac{1}{2} a \, \mathrm{e}^{\mathrm{i}kx}, \quad \zeta_{11} = \frac{\mathrm{i}k}{\omega} A_0 \sinh kh \, \mathrm{e}^{\mathrm{i}kx}, \tag{2.15}$$

where $a = 2\mathrm{i}\omega f'(h') A_0/g$. The dispersion relation is

$$\omega^4(\rho \coth kh \coth kh' + \rho') - \omega^2 \rho(\coth kh' + \coth kh) gk + (\rho - \rho') g^2 k^2 = 0. \tag{2.16}$$

Thus for a given k, there are two roots for ω^2; the larger root corresponds to the surface wave (barotropic) mode, while the smaller root to the internal wave (baroclinic) mode. Of later use is the limit of long waves where $kh, kh' \ll 1$. Equation (2.16) can be reduced to

$$\left(\frac{\omega}{k}\right)^4 - g(h+h')\left(\frac{\omega}{k}\right)^2 + \frac{\rho - \rho'}{\rho} g^2 hh' = 0, \tag{2.17a}$$

or

$$\left[\left(\frac{\omega}{k}\right)^2 - U_{\mathrm{S}}^2\right]\left[\left(\frac{\omega}{k}\right)^2 - U_{\mathrm{I}}^2\right] = 0. \tag{2.17b}$$

The two roots are simply,

$$\left\{\begin{matrix} U_{\mathrm{S}}^2 \\ U_{\mathrm{I}}^2 \end{matrix}\right\} = \tfrac{1}{2} g \left\{h + h' \pm \left[(h-h')^2 + 4hh' \frac{\rho'}{\rho}\right]^{\frac{1}{2}}\right\}, \tag{2.18}$$

where U_S and U_I are the phase velocities of the surface and internal modes respectively. Since the density difference is usually small

$$(\rho-\rho')\rho = \Delta\rho/\rho \ll 1, \tag{2.19}$$

we may approximate (2.18) by

$$U_S \approx [g(h+h')]^{\frac{1}{2}}, \quad U_I \cong [gh'(\Delta\rho/\rho)]^{\frac{1}{2}}(1+h'/h)^{-\frac{1}{2}}. \tag{2.20}$$

Throughout this paper the incident wavetrain is assumed to be of the surface wave mode corresponding to the larger root of (2.16).

3. Long waves locked to the progressive short waves

Conservation of mass in the lower layer requires, exactly, that

$$\zeta_t + \frac{\partial}{\partial x}\int_{-h}^{\zeta} u\,\mathrm{d}z + \frac{\partial}{\partial y}\int_{-h}^{\zeta} v\,\mathrm{d}z = 0. \tag{3.1}$$

Accurate to the order $O(\epsilon^2)$, the above equation may be approximated by

$$\zeta_t + \frac{\partial}{\partial x}\left\{\int_{-h}^{0} u\,\mathrm{d}z + [\zeta u]_{z=0}\right\} + \frac{\partial}{\partial y}\left\{\int_{-h}^{0} v\,\mathrm{d}z + [\zeta v]_{z=0}\right\} = O(\epsilon^3). \tag{3.2}$$

Substituting the expansions (2.8) and (2.9) and taking averages in time over $2\pi/\omega$ and in space over $2\pi/k$, we get,

$$\bar{\zeta}_{20t_1} + h\nabla_1^2\phi_{10} + \boldsymbol{\nabla}_1\cdot[\zeta_{11}^*\,\boldsymbol{\nabla}_h\phi_{11} + *]_{z=0} = 0, \tag{3.3}$$

where $\bar{\zeta}_{20}$ denotes the spatial average of ζ_{20}, $\boldsymbol{\nabla}_h = (\partial/\partial x, \partial/\partial y)$, $\boldsymbol{\nabla}_1 = (\partial/\partial x_1, \partial/\partial y_1)$ and $*$ denotes the complex conjugate of the preceding term in the same brackets. The potential ϕ_{10} can be shown to be independent of the short scales x, y, z and t (Agnon & Mei 1985). Although each term is associated with $O(\epsilon^3)$, there is no contribution to (3.3) by the omitted terms on the right-hand side of (3.2). Similarly, conservation of mass in the upper layer gives exactly

$$\zeta_t' - \zeta_t + \frac{\partial}{\partial x}\int_{\zeta}^{h'+\zeta'} u'\,\mathrm{d}z + \frac{\partial}{\partial y}\int_{\zeta}^{h'+\zeta'} v'\,\mathrm{d}z = 0, \tag{3.4}$$

which in turn gives

$$\bar{\zeta}_{20t_1}' - \bar{\zeta}_{20t_1} + h'\nabla_1^2\phi_{10} + \boldsymbol{\nabla}_1\cdot[\zeta_{11}'^*\,\boldsymbol{\nabla}_h\phi_{11}' + *]_{z=h} - \boldsymbol{\nabla}_1\cdot[\zeta_{11}^*\,\boldsymbol{\nabla}_h\phi_{11}' + *]_{z=0} = 0. \tag{3.5}$$

The potential ϕ_{10}' depends on the long scales only. Furthermore Bernoulli's equation implies

$$-g\bar{\zeta}_{20}' = \phi_{10t_1}' + [|\boldsymbol{\nabla}\phi_{11}'|^2 + (\mathrm{i}\omega\zeta_{11}'\,\phi_{11z}'^* + *)]_{z=h'}, \tag{3.6}$$

on the free surface, and

$$\rho'\{g\bar{\zeta}_{20} + \phi_{10t_1}' + [|\boldsymbol{\nabla}\phi_{11}'|^2 + (\mathrm{i}\omega\zeta_{11}\,\phi_{11z}'^* + *)]\} = \rho\{g\bar{\zeta}_{20} + \phi_{10t_1} + [|\boldsymbol{\nabla}\phi_{11}|^2 + (\mathrm{i}\omega\zeta_{11}\,\phi_{11_z}^* + *)]\}_{z=0}, \tag{3.7}$$

on the interface.

Let us assume the short surface waves to be modulated sinusoidally, i.e.

$$\zeta_{11}' = \left[\mathrm{Re}\,\tfrac{1}{2}a\exp-\mathrm{i}\Omega\left(t_1 - \frac{x_1}{C_g}\right)\right]\mathrm{e}^{\mathrm{i}kx}, \tag{3.8}$$

where C_g is the group velocity of the short wave. In view of the quadratic terms in (3.3), (3.5), (3.6), and (3.7) the long-wave response must have both a steady component independent of t_1 and a sinusoidal component in the following form

$$(\phi_{10}^{\mathrm{L}}, \phi'^{\mathrm{L}}_{10}, \zeta_{20}^{\mathrm{L}}, \bar{\zeta}'^{\mathrm{L}}_{20}) = \mathrm{Re}\,[(E, E', Z, Z')\tfrac{1}{2}A_0^2 \exp -2\mathrm{i}\Omega(t_1 - x_1/C_g)]. \tag{3.9}$$

The steady component corresponds to the set-down and will not be discussed here. The periodic component is just the locked long waves, denoted here by the superscript L. From (3.3), (3.5), (3.6) and (3.7), we easily obtain a matrix equation

$$\boldsymbol{N}\begin{Bmatrix} -2\mathrm{i}\Omega E \\ -2\mathrm{i}\Omega E' \\ Z \\ Z' \end{Bmatrix} = \begin{Bmatrix} \alpha_1 \\ \alpha_2 \\ \alpha_3 \\ \alpha_4 \end{Bmatrix}, \tag{3.10}$$

where the components on the right-hand side are

$$\begin{Bmatrix} \alpha_1 \\ \alpha_2 \\ \alpha_3 \\ \alpha_4 \end{Bmatrix} = k^2 \begin{Bmatrix} \dfrac{1}{\omega C_g} \sinh 2kh \\ \dfrac{1}{\omega C_g}\,[(B^2+C^2)\sinh 2kh' + 4BC \sinh^2 kh'] \\ \rho - \rho'(C^2 - B^2) \\ C^2 - B^2 \end{Bmatrix}. \tag{3.11}$$

The coefficient matrix in (3.10) is

$$\boldsymbol{N} = \begin{bmatrix} \dfrac{h}{C_g^2} & 0 & 1 & 0 \\ 0 & \dfrac{h'}{C_g^2} & -1 & 1 \\ -\rho & \rho' & -(\rho - \rho')g & 0 \\ 0 & -1 & 0 & -g \end{bmatrix}. \tag{3.12}$$

Its determinant can be reduced to

$$||\boldsymbol{N}|| = \frac{1}{C_g^4}\{\rho C_g^4 - \rho g(h+h')C_g^2 + (\rho - \rho')g^2 hh'\} \tag{3.13a}$$

$$= \frac{1}{C_g^4}\rho(C_g^2 - U_1^2)(C_g^2 - U_S^2), \tag{3.13b}$$

where U_1 and U_S are the phase speeds of equation (2.18). If the group velocity of the short waves is near U_1 or U_S, the matrix equation (3.10) is nearly singular, i.e. periodic groups of short waves can resonate either of these long waves. Of later use in this study are the amplitudes E, E' Z, and Z' which can be calculated by inverting the matrix. Some sample results for Z and Z' are plotted in figure 2 (a, b) as functions of kh' with h'/h as a parameter. The relative density difference is taken to be $\Delta\rho/\rho = 0.01$. Results for $\Delta\rho/\rho = 0.001$ are similar and are not shown here. Note that for $kh' \downarrow 0$, both locked long waves become unbounded since $C_g \downarrow U_S$. When kh' is

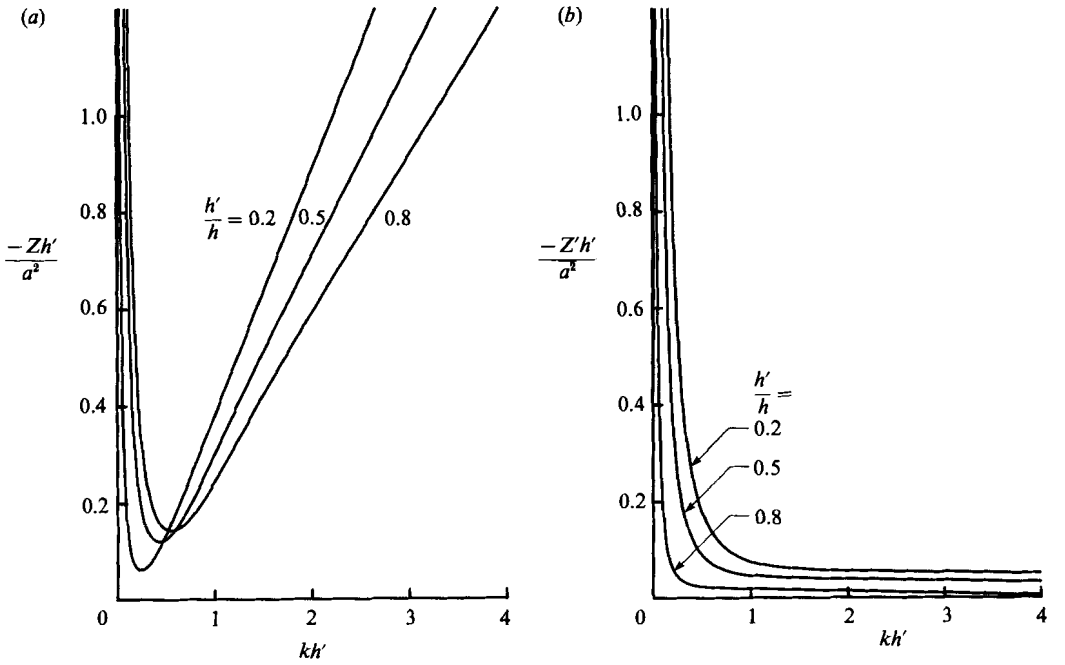

FIGURE 2. (*a*) Amplitude of the locked long wave on the free surface. (*b*) Amplitude of the locked long wave on the interface.

sufficiently large, $C_g \uparrow U_I$; the locked long interfacial wave becomes unbounded, but the locked long surface wave does not. While the initial tendency of resonance is evident in figure 2 (*b*), the immediate neighbourhood of resonance is beyond the range of kh' plotted here. Note that the matrix $\boldsymbol{N}$ and the α are independent of the modulational frequency Ω, therefore, ΩE, $\Omega E'$, Z and Z' are the same for all Ω. This means, in particular, that in the limit of uniform incident waves, $\Omega = 0$, these locked long waves also become steady set-downs.

To get bounded response near resonance, higher-order nonlinearity is needed in a treatment involving much longer time and space scales than are considered here. This was discussed in the works cited in §1. Our objective is to examine the effect of diffraction in the space and time domain of kx, ky, $\omega t = O(1/\epsilon)$.

4. The short-wave diffraction

For a uniform wavetrain the diffraction problem for a semi-infinite barrier has been solved exactly. But for our purposes the parabolic approximation is simpler and adequate. In this approximation we write ϕ_{11} and ϕ'_{11} as the sum of a right-going wave and a left-going wave with diffraction factors which are important near the rays passing the tip of the barrier. In the present case of normal incidence these critical rays all lie on the x-axis,

$$\begin{Bmatrix} \phi_{11} \\ \phi'_{11} \end{Bmatrix} = A \begin{Bmatrix} f(z) \\ f'(z) \end{Bmatrix} (\phi^+ \, e^{ikx} + \phi^- \, e^{-ikx}). \tag{4.1}$$

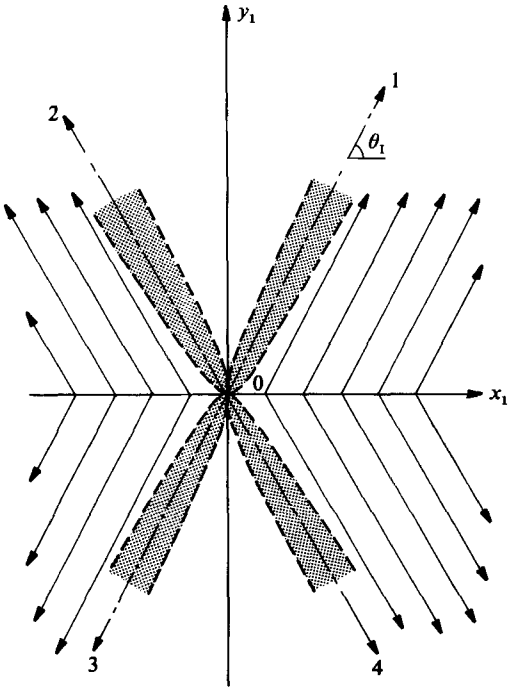

FIGURE 3. Radiation zones of free baroclinic long waves. Lines $\overline{01}$ and $\overline{04}$ are the bounding members of the family of rays emitted from the positive x-axis; $\overline{02}$ and $\overline{03}$ are the bounding members of the family of rays emitted from the negative x-axis.

where in f and f', (cf. (2.12) and (2.13)), ω and k are those of the short-surface-wave mode. According to the parabolic approximation (see e.g. Mei 1983), we have

$$\phi^+ = \begin{Bmatrix} D(-\sigma) \\ 1 \end{Bmatrix} \qquad \begin{Bmatrix} x > 0 \\ x < 0 \end{Bmatrix}, \tag{4.2}$$

and

$$\phi^- = \begin{Bmatrix} 0 \\ D(\sigma) \end{Bmatrix} \qquad \begin{Bmatrix} x > 0 \\ x < 0 \end{Bmatrix}, \tag{4.3}$$

where

$$D(\sigma) \approx \frac{1}{\sqrt{2}} \{\tfrac{1}{2} + C(\sigma) + \mathrm{i}[\tfrac{1}{2} + S(\sigma)]\}\, \mathrm{e}^{-\frac{1}{4}\mathrm{i}\pi}, \tag{4.4}$$

with

$$\sigma = ky/(\pi k|x|)^{\frac{1}{2}}, \tag{4.5}$$

C and S are Fresnel cosine and sine integrals. It is sufficient to note that

$$D(\sigma) \to 1 \quad \text{for } \sigma \to +\infty, \quad D(\sigma) \to 0 \quad \text{for } \sigma \to -\infty. \tag{4.6}$$

The approximation (4.1) is very good away from the sharp tip as long as $kr \gg 1$ where $r^2 = x^2 + y^2$, hence also where $kx_1 = O(1)$. The edge boundary layer, i.e. the near field of the x-axis, which is the transition strip of the shadow or of the reflection zone can be defined as

$$\sigma = ky/(\pi k|x|)^{\frac{1}{2}} = O(1). \tag{4.7}$$

Since for the long waves we are interested in the far field defined by $\epsilon kx = kx_1 = O(1)$ and $\epsilon ky = ky_1 = O(1)$, the width of the edge boundary layer is $ky = O(\epsilon^{-\frac{1}{2}})$ or $ky_1 = O(\epsilon^{\frac{1}{2}})$, and is small.

Taking into account the modulation of A in (4.1), the first-order short wave can be re-expressed as

$$\left.\begin{aligned}\phi_{11} &= f(z)\left\{\phi^+ A\left(t_1-\frac{x_1}{C_g}\right)e^{ikx}+\phi^- A\left(t_1+\frac{x_1}{C_g}\right)e^{-ikx}\right\},\\ \phi'_{11} &= f'(z)\left\{\phi^+ A\left(t_1-\frac{x_1}{C_g}\right)e^{ikx}+\phi^- A\left(t_1+\frac{x_1}{C_g}\right)e^{-ikx}\right\},\end{aligned}\right\} \tag{4.8}$$

where the envelope is given by

$$A(t_1) = \frac{ga}{2i\omega f'(h')}\cos\Omega t_1 = A_0\cos\Omega t_1. \tag{4.9}$$

Far outside of the edge boundary layer, $ky_1 = O(1)$, the factors ϕ^+, ϕ^- and D are either 0 or 1. The potentials ϕ_{11} and ϕ'_{11} are just plane waves modulated in x only. The corresponding locked long waves are right-going below the x-axis, zero in the first quadrant, and are two opposite-going waves with equal amplitudes in the second quadrant. This is summarized below,

$$\frac{\phi_{10}^{\mathrm{L}}}{E} = \frac{\phi_{10}'^{\mathrm{L}}}{E'} = \begin{cases} 0 & \text{in quadrant I}\\ \mathrm{Osc}\left\{\left|A\left(t_1-\frac{x_1}{C_g}\right)\right|^2+\left|A\left(t_1+\frac{x_1}{C_g}\right)\right|^2\right\} & \text{in quadrant II}\\ \mathrm{Osc}\left\{\left|A\left(t_1-\frac{x_1}{C_g}\right)\right|^2\right\} & \text{in quadrant III \& IV}\end{cases} \tag{4.10}$$

where Osc { } stands for 'the oscillatory part of { }. The amplitudes E and E' are obtained from (3.10). Clearly, by themselves these locked long waves are discontinuous across the x-axis. We must now examine the long period oscillations in the near field, i.e. in the edge boundary along the positive and negative x-axis and add free long waves in the far field $(kx_1, ky_1) = O(1)$.

5. Long period oscillations in the near field of the edge boundary layer

The near field is independent of y_1 and can be expanded in the manner of (2.8) and (2.9)

$$\Phi = \sum_{n=1}^{\infty}\epsilon^n\sum_{m=-n}^{n}\psi_{nm}e^{-im\omega t}, \quad \Phi' = \sum_{n=1}^{\infty}\epsilon^n\sum_{m=-n}^{n}\psi'_{nm}e^{-im\omega t}, \tag{5.1}$$

where the zeroth harmonics ψ_{n0} and ψ'_{n0} depend only on y, z, x_1 and t_1. From Laplace's equation and the boundary condition on the seabed we have for $n = 1, 2$,

$$\left(\frac{\partial^2}{\partial y^2}+\frac{\partial^2}{\partial z^2}\right)\begin{pmatrix}\psi_{n0}\\ \psi'_{n0}\end{pmatrix} = 0 \quad \begin{matrix}(-h<z<0),\\ (0<z<h'),\end{matrix} \tag{5.2}$$

$$\frac{\partial\psi_{n0}}{\partial z} = 0 \quad (z=-h). \tag{5.3}$$

Taylor expansion of the kinematic condition on the free surface at $z = h'+\zeta'$ gives,

$$\zeta'_t = \Phi'_z+\zeta'\Phi'_{zz}-\Phi'_x\zeta'_x-\Phi'_y\zeta'_y+O(\epsilon^3) = \Phi'_z-\nabla_h\cdot(\zeta'\nabla_h\Phi')+O(\epsilon^3) \quad (z=h'). \tag{5.4}$$

Inserting (5.1) into this we obtain at the first order,

$$\psi'_{10_z} = 0 \quad (z = h'), \tag{5.5}$$

and at the second order

$$g\psi'_{20z} = \nabla_h \cdot [\mathrm{i}\omega\psi'_{11}\nabla_h\psi'^{*}_{11} + *] = \nabla_h \cdot [\mathrm{i}\omega\psi'_{11}\nabla_h\psi'^{*}_{11} - \mathrm{i}\omega\psi'^{*}_{11}\nabla_h\psi'_{11}]$$
$$= \mathrm{i}\omega\psi'_{11}\nabla_h^2\psi'^{*}_{11} - \mathrm{i}\omega\psi'^{*}_{11}\nabla_h^2\psi'_{11} = \mathrm{i}\omega\psi'_{11}[-k^2\psi'^{*}_{11}] - \mathrm{i}\omega\psi'_{11}[-k^2\psi'^{*}_{11}] = 0 \quad (z = h'). \tag{5.6}$$

In deducing the last equality we have used the fact that ψ'_{11} involves only propagating waves and satisfies the Helmholtz equation in the (x, y)-plane. It follows that

$$\psi'_{20z} = 0 \quad (z = h'), \tag{5.7}$$

also. Similar consideration at the interface gives

$$\psi'_{20_z} = \psi_{20_z} = 0 \quad (z = 0). \tag{5.8}$$

Thus the most general near field solution for the zeroth harmonic up to $O(\epsilon^2)$ is,

$$\psi = \epsilon\psi_{10} + \epsilon^2\psi_{20} \quad \text{with}\ \psi_{n0} = b_n + c_n y \quad (n = 1, 2), \tag{5.9}$$

where b_n and c_n are unknown functions of x_1, and t_1 only. The corresponding solutions in the upper layer are similar.

Now the near field solution $\epsilon\psi_{10} + \epsilon^2\psi_{20}$ must be matched asymptotically with the far field, i.e.

$$[\phi_{10}]_{0+} + y_1\left[\frac{\partial\phi_{10}}{\partial y_1}\right]_{0+} = \psi_{10} + \epsilon\psi_{20} = [\phi_{10}]_{0-} + y_1\left[\frac{\partial\phi_{10}}{\partial y_1}\right]_{0-}, \tag{5.10}$$

where $[\ ]_{0+}$ means the limit of $[\ ]$ as $y_1 \to 0+$. Equation (5.10) can be satisfied if

$$c_1 = 0, \quad b_2 = 0, \tag{5.11}$$

throughout the near field, and if

$$\phi_{10}(x_1, y_1 = 0^+, t_1) = b_1 = \psi_{10}(x_1, t_1) = \phi_{10}(x_1, y_1 = 0^-, t_1), \tag{5.12}$$

and

$$\phi_{10y_1}(x_1, y_1 = 0^+, t_1) = c_2 = \psi_{20_y} = \phi_{10y_1}(x_1, y_1 = 0^-, t_1). \tag{5.13}$$

Two similar equations hold for the upper layer. Thus the near field is effectively transparent to the long wave and matching is made directly between the far field potentials on both sides of the shadow and reflection edges.

6. The free long waves

The total slow potential in the far field is the sum of locked and free long waves:

$$\phi_{10} = \phi_{10}^{\mathrm{L}} + \phi_{10}^{\mathrm{F}}, \quad \phi'_{10} = \phi'^{\mathrm{L}}_{10} + \phi'^{\mathrm{F}}_{10}. \tag{6.1}$$

The potentials for the free long waves, distinguished by the superscript F, are governed by the homogeneous versions of (3.3), (3.5), (3.6) and (3.7), i.e.

$$\bar{\zeta}^{\mathrm{F}}_{20t_1} + h\nabla_1^2\phi^{\mathrm{F}}_{10} = 0, \quad \bar{\zeta}'^{\mathrm{F}}_{20t_1} - \bar{\zeta}^{\mathrm{F}}_{20t_1} + h'\nabla_1^2\phi'^{\mathrm{F}}_{10} = 0, \tag{6.2a, b}$$

$$-g\bar{\zeta}'^{\mathrm{F}}_{20} = \phi'^{\mathrm{F}}_{10t_1}, \quad \rho'(g\bar{\zeta}^{\mathrm{F}}_{20} + \phi'^{\mathrm{F}}_{10t_1}) = \rho(g\bar{\zeta}^{\mathrm{F}}_{20} + \phi^{\mathrm{F}}_{10t_1}). \tag{6.2c, d}$$

Eliminating $\bar{\zeta}_{20}$ and $\bar{\zeta}'_{20}$ yields

$$\left(\frac{\partial^2}{\partial t_1^2}-U_1^2\nabla_1^2\right)\left(\frac{\partial^2}{\partial t_1^2}-U_S^2\nabla_1^2\right)\begin{bmatrix}\phi'^{\mathrm{F}}_{10}\\ \phi^{\mathrm{F}}_{10}\end{bmatrix}=0. \tag{6.3}$$

From (5.12) and (5.13) we get the boundary conditions:

$$\phi^{\mathrm{F}}_{10}|^{y_1=0^+}_{y_1=0^-}=-\phi^{\mathrm{L}}_{10}|^{y_1=0^+}_{y_1=0^-}=\pm E\ \mathrm{Osc}\left\{\left|A\left(t_1\mp\frac{x_1}{C_g}\right)\right|^2\right\}\qquad (x_1\gtrless 0), \tag{6.4a}$$

$$\phi'^{\mathrm{F}}_{10}|^{y_1=0^+}_{y_1=0^-}=-\phi'^{\mathrm{L}}_{10}|^{y_1=0^+}_{y_1=0^-}=\pm E'\ \mathrm{Osc}\left\{\left|A\left(t_1\mp\frac{x_1}{C_g}\right)\right|^2\right\}\qquad (x_1\gtrless 0), \tag{6.4b}$$

$$\phi^{\mathrm{F}}_{10y_1}|^{y_1=0^+}_{y_1=0^-}=-\phi^{\mathrm{L}}_{10y_1}|^{y_1=0^+}_{y_1=0^-}=0\qquad (\mathrm{all}\ x_1), \tag{6.4c}$$

$$\phi'^{\mathrm{F}}_{10y_1}|^{y_1=0^+}_{y_1=0^-}=-\phi'^{\mathrm{L}}_{10y_1}|^{y_1=0^+}_{y_1=0^-}=0\qquad (\mathrm{all}\ x_1). \tag{6.4d}$$

Use has been made of (4.10).

From (6.4*a*, *b*) and (6.4*c*, *d*), we immediately see that ϕ^{F}_{10} and ϕ'^{F}_{10} are antisymmetric in x_1. From (6.4*c*, *d*) and the form of the solution to be stated shortly (6.9), ϕ^{F}_{10} and ϕ'^{F}_{10} are also antisymmetric in y_1. It is therefore mathematically sufficient to solve for the free long waves in any of the four quadrants. Accordingly, we choose to consider the first quadrant only. Furthermore we need the boundary conditions along the barrier

$$\phi^{\mathrm{F}}_{10x_1}=\phi'^{\mathrm{F}}_{10x_1}=0\quad\text{on}\quad x_1=0,\quad y_1\geqslant 0, \tag{6.5}$$

and along the positive x-axis (shadow edge)

$$\begin{Bmatrix}\phi'^{\mathrm{F}}_{10}\\ \phi^{\mathrm{F}}_{10}\end{Bmatrix}=\tfrac{1}{2}\mathrm{Re}\begin{Bmatrix}E'\\ E\end{Bmatrix}A_0^2\exp\left[-2\mathrm{i}\Omega\left(t_1-\frac{x_1}{C_g}\right)\right]\quad (x_1\geqslant 0,\quad y_1=0). \tag{6.6}$$

We expect the free-wave displacements $\bar{\zeta}^{\mathrm{F}}_{20}$ and $\bar{\zeta}'^{\mathrm{F}}_{20}$ to have the same dependence on t_1 and x_1. Being homogeneous solutions of (6.3), the free long waves are a linear combination of surface (barotropic) and internal (baroclinic) modes. They must therefore have the total wavenumbers $2\Omega/U_S$ and $2\Omega/U_I$ respectively. Because U_I is usually much smaller than U_S, under a wide range of conditions the wavenumber of the free long waves in the x-direction $2\Omega/C_g$ may lie between them,

$$\frac{2\Omega}{U_S}<\frac{2\Omega}{C_g}<\frac{2\Omega}{U_I}. \tag{6.7}$$

Assuming this inequality, the free internal waves will have real and finite wave numbers in the y_1-direction also, while the y_1-component of the free-surface wavenumber is imaginary, implying that the surface mode is evanescent in the y_1-direction. Thus the free internal waves must be inclined in the direction

$$\theta_I=\cos^{-1}\frac{U_I}{C_g}, \tag{6.8}$$

with respect to the x-axis and propagate into the shadow. In all four quadrants, internal waves are radiated from the x-axis symmetrically in four directions, as sketched in figure 3. In the sense of geometrical optics, these free internal waves are bounded by the four rays $\overline{01}$, $\overline{02}$, $\overline{03}$ and $\overline{04}$ in figure 3. For small density difference and $kh'=O(1)$, U_I/C_g can be very small (cf. 2.20). The angle θ_I is then close to $\frac{1}{2}\pi$;

thus the crests of the free baroclinic wave of long period are nearly perpendicular to the barrier. On the other hand, if $U_1/C_g \approx 1$ for any reason, then $\theta_1 \approx 0$, implying that the resonated internal wave does not penetrate the shadow. Therefore shadow penetration and resonance do not occur together and the present second-order analysis is adequate for the former.

We now give the formal solution of the free long wave potential between the rays $\overline{01}$, $\overline{02}$. $\overline{03}$ and $\overline{04}$. In compact notation, they are

$$\phi_{10}^{\mathrm{F}} \sim (\operatorname{sgn} x_1)(\operatorname{sgn} y_1)\operatorname{Re}\left[\phi_{\mathrm{S}} \exp\left(-2\mathrm{i}\Omega\left(t_1 - \frac{|x_1|}{C_g} - \mathrm{i}\nu_{\mathrm{S}}|y_1|\right)\right) + \phi_{\mathrm{I}} \exp\left(-2\mathrm{i}\Omega\left(t_1 - \frac{|x_1|}{C_g} - \nu_{\mathrm{I}}|y_1|\right)\right)\right], \quad (6.9a)$$

$$\phi_{10}'^{\mathrm{F}} \sim (\operatorname{sgn} x_1)(\operatorname{sgn} y_1)\operatorname{Re}\left[\phi_{\mathrm{S}}' \exp\left(-2\mathrm{i}\Omega\left(t_1 - \frac{|x_1|}{C_g} - \mathrm{i}\nu_{\mathrm{S}}|y_1|\right)\right) + \phi_{\mathrm{I}}' \exp\left(-2\mathrm{i}\Omega\left(t_1 - \frac{|x_1|}{C_g} - \nu_{\mathrm{I}}|y_1|\right)\right)\right], \quad (6.9b)$$

which satisfy (6.4*c*) and (6.4*d*) respectively. The coefficients ϕ_{S}, ϕ_{S}', ϕ_{I} and ϕ_{I}' are to be determined. Physically $\phi_{\mathrm{S}}(\phi_{\mathrm{S}}')$ corresponds to the barotropic mode in the lower (upper) layer, while $\phi_{\mathrm{I}}(\phi_{\mathrm{I}}')$ corresponds to the baroclinic mode in the lower (upper) layer. The wavenumbers in the y-directions are $\mathrm{i}\nu_{\mathrm{S}}$ and ν_{I}, where:

$$-\nu_{\mathrm{S}}^2 + \frac{1}{C_g^2} = \frac{1}{U_{\mathrm{S}}^2}, \quad \nu_{\mathrm{I}}^2 + \frac{1}{C_g^2} = \frac{1}{U_{\mathrm{I}}^2}. \quad (6.10)$$

Note that ν_{S} and ν_{I} are both real because of (6.7) and that the barotropic mode is exponentially attenuating with y_1. Near any limiting ray, say, $\overline{01}$, there is a parabolic boundary layer within which ϕ_{10}^{F} and $\phi_{10}'^{\mathrm{F}}$ are modified by the diffraction factor $D(\hat{\sigma})$ with

$$\hat{\sigma} = -K\hat{y}_1/(\pi K|\hat{x}_1|)^{\frac{1}{2}} \quad (K = 2\Omega/U_1), \quad (6.11)$$

and $(\hat{x}_1, \hat{y}_1)$ is a Cartesian coordinate system with $\hat{x}_1$ coinciding with the ray $\overline{01}$

$$\begin{Bmatrix}\hat{x}_1\\ \hat{y}_1\end{Bmatrix} = \begin{bmatrix}\cos\theta_{\mathrm{I}} & \sin\theta_{\mathrm{I}}\\ -\sin\theta_{\mathrm{I}} & \cos\theta_{\mathrm{I}}\end{bmatrix}\begin{Bmatrix}x_1\\ y_1\end{Bmatrix}. \quad (6.12)$$

The product of the diffraction factor D and the potential in (6.9*a*) describes the 'radiated' free long-wave field in the first quadrant ($x_1, y_1 > 0$). The free waves elsewhere can be simply inferred by antisymmetry with respect to both x_1 and y_1. Since in general these waves propagate away from the y_1-axis, the boundary conditions (6.5) are ineffective. In case θ_{I} is nearly $\frac{1}{2}\pi$, (6.5) is then automatically satisfied.

It now remains to determine the amplitude of the free waves ϕ_{S}, ϕ_{S}', ϕ_{I} and ϕ_{I}'. We first find from (6.2*a–d*) the ratio of the amplitudes of the potentials for the two modes. For the surface mode of the free long-waves, we replace the operator ∇_1^2 in (6.2*a*, *b*) by $U_{\mathrm{S}}^{-2}\partial^2/\partial^2 t_1^2$, eliminate $\bar{\zeta}_{20}'^{\mathrm{F}}$ and $\bar{\zeta}_{20}^{\mathrm{F}}$ with the help of (6.2*c*) and then integrate the result with respect to t_1. The ratio $\phi_{\mathrm{S}}/\phi_{\mathrm{S}}'$ is thus determined:

$$\frac{\phi_{\mathrm{S}}}{\phi_{\mathrm{S}}'} = \frac{U_{\mathrm{S}}^2 - gh'}{gh} > 0. \quad (6.13)$$

Replacing U_S^2 by U_I^2, we get for the internal free wave mode:

$$\frac{\phi_I}{\phi_I'} = \frac{U_I^2 - gh'}{gh} < 0. \tag{6.14}$$

These relations are of course well known. Applying (6.4a, b) to (6.9) we have:

$$\phi_I + \phi_S = \tfrac{1}{2}EA_0^2, \quad \phi_I' + \phi_S' = \tfrac{1}{2}EA_0^2. \tag{6.15a, b}$$

Equations (6.13) to (6.15) can be immediately solved to give ϕ_I, ϕ_S, ϕ_I' and ϕ_S'. The results are:

$$\phi_S' = \frac{\frac{1}{2}gh}{U_S^2 - U_I^2}\left\{E - E'\left(\frac{U_I^2 - gh'}{gh}\right)\right\}\tfrac{1}{2}A_0^2, \tag{6.16a}$$

$$\phi_I = \frac{U_I^2 - gh'}{2(U_S^2 - U_I^2)}\left\{E - E'\left(\frac{U_S^2 - gh'}{gh}\right)\right\}\tfrac{1}{2}A_0^2, \tag{6.16b}$$

where E and E' are obtained from the solution of (3.10). ϕ_S and ϕ_I' then follow from (6.13) and (6.14). The corresponding interface displacements are found from (6.2a). By defining ζ_S and ζ_I from $\bar{\zeta}_{20}^F$ in the manner of (6.9) we easily find, in particular, the free baroclinic component of the interfacial displacement:

$$\zeta_I = \frac{2i\Omega h}{U_I^2}\phi_I. \tag{6.17}$$

For the same mode, the free surface displacement ζ_I' is smaller than ζ_I by a factor of $O(\Delta\rho/\rho)$ and is insignificant. In view of the discussion of figure 2 and (2.18) $\Omega \cdot (\phi_S, \phi_S', \phi_I, \phi_I')$ are independent of Ω. It follows that ζ_I is the same for all Ω. In the limit of unmodulated short waves $\Omega = 0$ starting from rest, ζ_I adds to the steady set-down on the interface.

Figure 4 shows some values of ζ_I, normalized as $-\bar{\zeta}_I = -\zeta_I h'/a^2$, *vs.* kh' for three different values of h'/h and $\Delta\rho/\rho = 0.01$. Results for $\Delta\rho/\rho = 0.001$ are again found to be similar, hence omitted. As in the case of locked long waves, $-\bar{\zeta}_I$ increases for decreasing h'/h. For very small kh', it can be shown analytically from (3.10)–(3.11) and (6.16)–(6.17) that ζ_I remains finite even though E and E' become unbounded. This is because resonance is associated with the barotropic mode while ζ_I is the baroclinic mode; a detailed proof of this is given in the Appendix. As kh' increases, $-\bar{\zeta}_I$ increases because of the initial approach to resonance as $C_g \uparrow U_I$. Nevertheless for a sufficiently wide range of kh' the quantitative results of $-\bar{\zeta}_I$ are still consistent with the second-order approximation employed here. Thus, while a long barrier may provide a shield against short surface waves, it may induce long internal waves that enter the geometrical shadow. This effect is a combined consequence of linear diffraction, nonlinearity and the special dispersive nature of the two-layered system (cf. (6.7)).

Finally, it is useful to have some quantitative idea about the circumstances where the mechanism of this paper is relevant. In a large laboratory basin (50 m wide × 50 m long, say), we may choose $h' = h = 0.3$ m, $\Delta\rho/\rho = 0.1$ and the incident surface-wave frequency $\omega = 2\pi/T = 10$ Hz. The following values for the short surface wave are than implied: $kh' = 3.3$, and $C_g = 0.8$ m/s. The phase speed of the free internal wave is $U_I = 0.39$ m/s according to (2.20). If we choose the group period to be $50T$, the frequency of the long internal wave is then $2\Omega = 0.4$ Hz. The wavelength should be $\lambda_I = 6.3$ m, corresponding to $k_I h' = k_I h = 0.3$. Thus the second-order internal wave is approximately of the shallow-water type and the

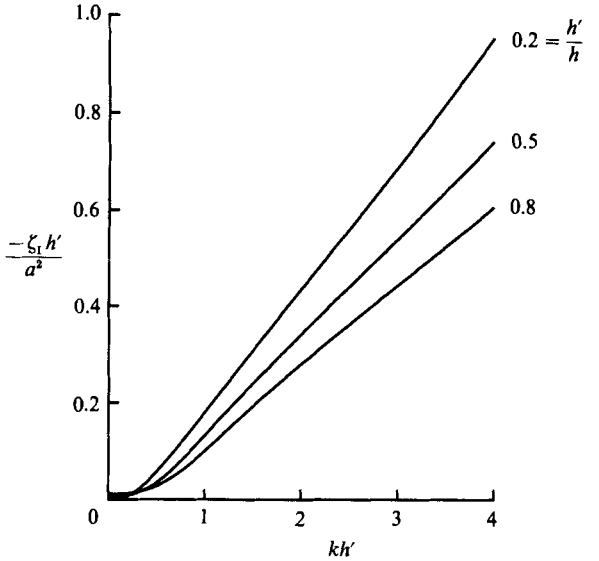

FIGURE 4. Normalized amplitude of free baroclinic long waves.

present theory should be verifiable directly by experiments. In an estuary the following values are possible, $\omega = 1$ Hz ($T = 2\pi$ s), $h' = 10$ m, $h = 20$ m, and $\Delta\rho/\rho = 0.01$. These imply $kh' = 1$, $C_g = 5$ m/s and a wavelength of $\lambda = 20\pi$ m. The phase speed of the free baroclinic wave is now $U_I = 0.8$ m/s. If $T_I = 100\,T = 200\pi$ s, then the wavelength is $\lambda_I = 240$ m (i.e. $kh' = 0.25$), which is rather long compared to h' but not quite so long compared to h. In this case the present theory can give only a crude quantitative estimate. Also, in an ocean the group period is likely to be much shorter than $100T$, and the density constant $\Delta\rho/\rho$ is much smaller than 0.01. Hence the second-order baroclinic waves are then not necessarily in shallow water. The present theory must be modified for quantitative accuracy. Lastly, the barrier can be either a floating structure or a natural barrier of more complex geometry. While the details of diffraction may change, the main feature of shadow penetration should remain.

Invasion of long waves, which are generated by interacting short waves, into zones where short waves cannot penetrate may occur in other circumstances also. For example, by Bragg resonance, modulated short surface waves can be substantially reflected by a large number of periodically spaced parallel bars, but free long waves are found to be prominent on the transmission side (Hara & Mei 1987). Although for a homogeneous fluid, no long wave can leak into the shadow of a semi-infinite barrier, certain changes of lateral boundaries and hence of the diffraction pattern of the short waves can result in long-wave penetration. An example of engineering interest is a fishing harbour with a small entrance. While wind-induced surface waves of $O(10$ s) period may be largely kept outside the harbour, long waves of $O(1$–5 min) period generated within by nonlinearity may be enhanced by harbour resonance. These possibilities bear partial resemblance to surf beats (here without the surf), and are worthy of further theoretical and experimental investigations.

We are grateful for the financial support of the Fluid Mechanics Program of the US Office of Naval Research (N00014-87-K-0121) and National Science Foundation (Grant MSM 851 4919). We thank the referees for their helpful comments.

Appendix. The limit of ζ_I as $kh' \downarrow 0$

Eliminating Z and E' among the first, second and the fourth of (3.10), we get

$$-2i\Omega hE + (C_g^2 - gh')\, Z = C_g^2(\alpha_1 + \alpha_2) + h'\alpha_4.$$

Now we eliminate Z and E' among the first, third and fourth of (3.10) to get

$$-2i\Omega\left(\Delta\rho \frac{gh}{C_g^2} - \rho\right) E - \rho' g Z' = \Delta\rho g\alpha_1 + \alpha_3 + \rho'\alpha_4.$$

The last two equations may be solved to give:

$$\begin{Bmatrix} 2i\Omega E \\ Z' \end{Bmatrix} = \begin{bmatrix} R_{11} & R_{12} \\ R_{21} & R_{22} \end{bmatrix}^{-1} \begin{Bmatrix} Q_1 \\ Q_2 \end{Bmatrix},$$

where

$$R_{11} = h, \qquad R_{12} = C_g^2 - gh',$$
$$R_{21} = \Delta\rho \frac{gh}{C_g^2} - \rho, \qquad R_{22} = -\rho' g,$$
$$Q_1 = C_g^2(\alpha_1 + \alpha_2) + h'\alpha_4, \quad Q_2 = \Delta\rho g a_1 + a_3 + r' a_4.$$

We may now calculate the braces { } in (6.16 *b*), using the fourth of (3.1):

$$F = -2i\Omega(E - \beta E') = \alpha_4\beta + \frac{Q_2(g\beta R_{11} - R_{12})}{D} + \frac{Q_1(R_{22} - g\beta R_{21})}{D},$$

where $\beta = \dfrac{U_S^2 - gh'}{gh}$, $D = R_{11}R_{22} - R_{12}R_{21} = \rho C_g^{-2}(C_g^2 - U_S^2)(C_g^2 - U_I^2)$.

Afte eliminating the factor $C_g^2 - U_s^2$, we get

$$F = \alpha_4\beta + \frac{Q_1(\Delta\rho/\rho - U_I^2/gh) - Q_2 C_g^2/\rho}{C_g^2 - U_I^2},$$

which is finite at $k = 0$. The corresponding limit of S_I is,

$$\zeta_I = \frac{-2i\Omega h}{U_I^2} \frac{gh' - U_I^2}{U_S^2 - U_I^2} (E - \beta E')^{\frac{1}{2}}$$
$$\to \tfrac{1}{2}k^2 A_0^2 \frac{(gh' - U_I^2)}{U_I^2(U_S^2 - U_I^2)} \left[\frac{U_S^2 - gh'}{g} + \frac{\Delta\rho\, U_S^2 h + (\Delta\rho\, gh - \rho U_I^2)\, h'}{\rho'(U_S^2 - U_I^2)}\right].$$

Note from (2.15) that kA_0 is proportional to the surface wave amplitude a which is kept constant as $k \downarrow 0$. This formula has been used to check the computations in figure 4.

REFERENCES

Agnon, Y. & Mei, C. C. 1985 Slow drift motions of a rectangular block in beam seas. *J. Fluid Mech.* **151**, 279–294.

Ball, F. K. 1974 Energy transfer between external and internal gravity waves. *J. Fluid Mech.* **19**, 465–478.

Dysthe, K. B. & Das, K. P. 1981 Coupling between a surface-wave spectrum and an internal wave: modulational interaction. *J. Fluid Mech.* **104**, 483–503.

HARA, T. & MEI, C. C. 1987 Bragg scattering of surface waves by periodic bars: theory and experiment. *J. Fluid Mech.* **178**, 221–242.

JOYCE, T. M. 1974 Nonlinear interactions among standing surface and internal gravity waves. *J. Fluid Mech.* **63**, 801–825.

LAMB, H. 1932 *Hydrodynamics*. Dover.

LEWIS, J. E., LAKE, B. M. & KO, D. R. S. 1974 On the interaction of internal waves and surface gravity waves. *J. Fluid Mech.* **63**, 773–800.

MEI, C. C. 1983 *The Applied Dynamics of Ocean Surface Waves*. Wiley-Interscience.

THORPE, S. A. 1966 On wave interactions in a stratified flow. *J. Fluid Mech.* **24**, 737–751.